ACKNOWLEDGMENT

The authors would like to thank the National Chip Implementation Center (CIC) for the chip fabrication and technical supports.

REFERENCES

1. Y.-J.E. Chen, Y.-J. Lee, and Y.-H. Yu, Investigation of polysilicon thin-film transistor technology for RF applications, IEEE Trans Microwave Theory Tech 58 (2010), 3444–3451.
2. T.-H. Lin, C.-L. Ti, and Y.-H. Liu, Dynamic current- matching charge pump and gated-offset linearization technique for delta-sigma fractional-N PLLs, IEEE Trans Circuits Syst 56 (2009), 877–885.
3. P. Park, D. Park, and S. Cho, A 2.4 GHz fractional-N frequency synthesizer with high-OSR ΔΣ modulator and nested PLL, IEEE J Solid-State Circuits 47 (2012), 2433–2443.
4. C.-T. Lu, H.-H. Hsieh, and L.-H. Lu, A low-power quadrature VCO and its application to a 0.6-V 2.4-GHz PLL, IEEE Trans Circuits Syst I 57 (2010), 793–802.
5. Y.-W. Chen, Y.-H. Yu, and Y.-J. Emery Chen, A 0.18-μm CMOS dual-band frequency synthesizer with spur reduction calibration, IEEE Microwave Wireless Compon Lett 23 (2013), 551–553.
6. T.-H. Lin and W.J. Kaiser, A 900-MHz 2.5 mA CMOS frequency synthesizer with an automatic SC tuning loop, IEEE J Solid-State Circuits 36 (2001), 424–431.
7. W.-H. Chen, W.-F. Loke, and B. Jung, A 0.5-V, 440-μW frequency synthesizer for implantable medical devices, IEEE J Solid-State Circuits 47 (2012), 1896–1907.
8. T.-W. Liao, J.-R. Su, and C.-C. Hung, Spur-reduction frequency synthesizer exploiting randomly selected PFD, IEEE Trans VLSI Syst 21 (2013), 589–592.
9. T.-W. Liao, C.-M. Chen, J.-R. Su, and C.-C. Hung, Random pulse-width matching frequency synthesizer with sub-sampling charge pump, IEEE Trans Circuits Syst I 59 (2012), 2815–2824.
10. K.-H. Cheng, Y.-C. Tsai, and Y.-L. Lo, A 0.5-V 0.4-2.24 GHz inductorless phase-locked loop in a system-on-chip, IEEE Trans Circuits Syst I 58 (2011), 849–859.
11. B. Zhao, Y. Lian, and H. Yang, A low-power fast- settling bond-wire frequency synthesizer with a dynamic-bandwidth scheme, IEEE Trans Circuits Syst I 60 (2013), 1188–1199.

SIW-BASED INTERDIGITAL BANDPASS FILTER WITH HARMONIC SUPPRESSION

Sinan Kurudere[1] and Vakur B. Ertürk[2]
[1] Meteksan Defence Ind. Inc., Ankara 06800, Turkey
[2] Department of Electrical and Electronics Engineering, Bilkent University, Ankara 06800, Turkey; Corresponding author: vakur@ee.bilkent.edu.tr

Received 9 June 2014

ABSTRACT: *A novel configuration of interdigital bandpass filter based on the substrate integrated waveguide (SIW) technology is proposed. In addition to the interdigital resonators in SIW that determine the main response/characteristics of the filter, narrowing the width of the SIW at the center of the filter and additional vias at its input and output parts act as two additional control mechanisms to achieve the desired filter response. Moreover, dumbbells are etched to the ground side of the microstrip feeding sections at both ends of the filter to improve its harmonic suppression. A prototype filter is designed and fabricated for verification. The measured results are in good agreement with the simulations, and the filter exhibits very good harmonic suppression.* © 2015 Wiley Periodicals, Inc. Microwave Opt Technol Lett 57:66–69, 2015; View this article online at wileyonlinelibrary.com. DOI 10.1002/mop.28782

Key words: *substrate integrated waveguide; interdigital resonator; harmonic suppression*

1. INTRODUCTION

Combline and interdigital type bandpass filters (BPFs) have been widely used in various microwave and millimeter wave applications due to their compactness, good stopband and selectivity performance, and relative ease of integration [1,2].Conversely, the substrate integrated waveguide (SIW) technology, formed using two linear arrays of metal vias embedded in a dielectric substrate to connect two metal plates (and hence, forming the electric sidewalls of the waveguide), has been proven to be useful to design compact size, high performance, low-cost integrated waveguide filters [3–9]. Therefore, realization of SIW-based combline and interdigital BPFs are important and can meet the stringent filtering requirements of recent wireless communication and radar applications [10].

Recently, capacitive posts are integrated within SIW cavities [11,12] to realize combline resonators in SIW technology, which are then used to design an X-band SIW-based combline BPF in [13]. In this article, similar resonators to the ones presented in [13] are used to design a novel SIW-based interdigital BPF, where each resonator is configured reversely with respect to the adjacent one within the SIW cavity (and hence, forms interdigital type SIW resonators). These interdigital SIW resonators determine the main response of the filter. However, two additional control mechanisms, namely, narrowing the width of the SIW at the middle of the filter and use of additional vias at its input and output parts, are introduced to achieve the desired filter response. Moreover, dumbbells are etched to the ground side of the microstrip feeding at both ends of the filter to improve its harmonic suppression. A third-order prototype BPF with a center frequency of 9 GHz and a 500 MHz bandwidth is designed and fabricated for verification. The measured results are in good agreement with the simulations, and the filter exhibits very good harmonic suppression with its compact size.

In Section 2, the design of the SIW-based interdigital BPF is given together with simulations supported by measurement results. Section 3 provides a detailed discussion on the improvements of the filter's harmonic suppression accompanied by the experimental results of the final design.

2. FILTER DESIGN

The structure of the proposed SIW-based interdigital filter, which uses a tapered microstrip-to-SIW transition at both its input and output ports, is shown in Figure 1 together with a picture of the fabricated prototype. After determining the width of the SIW (a_s), diameter of the vias (d), and center-to-center separation between the vias (p) along the longitudinal direction using the empirical design equations given in [3], a combline type resonator, similar to the one presented in [13] and shown in Figure 2 is designed, which forms the main building block of the filter. This resonator is formed from a metallic via short-circuited at the bottom metallization and open-ended with a cap (a metallic disk) at the top metallization. The radius of the cap mainly determines the upper cutoff frequency (f_c^u) of the passband. As its radius increases, the f_c^u shifts to a lower frequency, and vice versa. An annular gap (see Fig. 2) is introduced on the top metal to separate the cap from the rest of the metallization establishing a capacitance between the cap and the metallization of the SIW through the fringing fields. Its size should be as small as possible to minimize potential radiation losses and is determined by the fabrication capability of our facility, which is 0.254 mm.

The order of the filter is determined from the number of the resonators, and because an interdigital type filter is designed, each resonator is configured reversely with respect to the

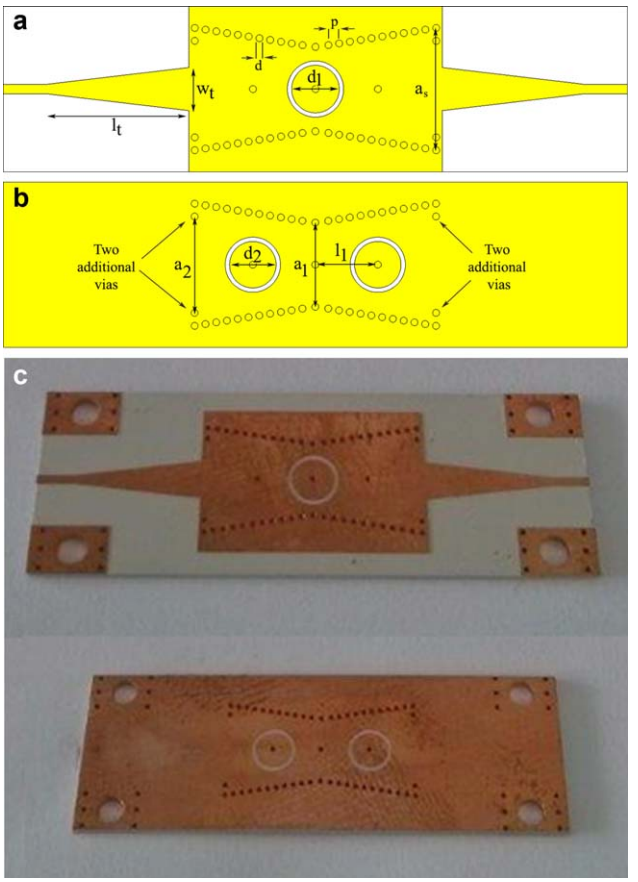

Figure 1 The structure of the proposed filter together with its fabricated prototype. (a) Top surface, (b) bottom surface, and (c) top and bottom surfaces of the fabricated prototype. [Color figure can be viewed in the online issue, which is available at wileyonlinelibrary.com]

adjacent one. For example, for a third-order filter shown in Figure 1, the cap of the middle resonator (i.e., the second resonator) together with the corresponding annular gap are on the top metallic surface of the SIW whereas the caps of the left and right resonators (i.e., the first and the third resonators) together with their corresponding annular gaps are on the bottom (i.e., ground) metallic surface of the filter. Note that combline and interdigital filters are symmetric. Therefore, again referring to the third-order filter depicted in Figure 1, the dimensions of the left and right resonators and their center-to-center distance from the middle resonator are the same. Two important design issues related to the proposed filter must be empasized at this point. First, the center-to-center distance between the resonators mainly affects the bandwidth of the filter (the larger the separation, the smaller the bandwidth, and vice versa). Second, during the initial design the cap radii of all the resonators are selected to be the same. However, to improve the matching, the cap radius of the middle resonator is adjusted (slightly different) at the fine-tuning stage of the final design.

Apart from the resonators, two additional control mechanisms, namely, narrowing the width of the SIW at the middle of the filter and use of additional vias at its input and output parts, are introduced to achieve the desired filter response. In addition to providing an extra control on the bandwidth and on the center frequency (f_0) of the fiter, these mechanisms help to establish a good matching as well as to obtain a symmetric filter response.

The first additional control mechanism is to narrow the width of the filter at its middle along the longitudinal direction as seen

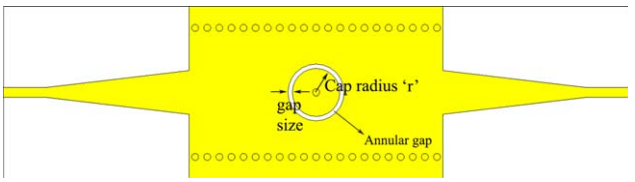

Figure 2 Single resonator in the SIW. [Color figure can be viewed in the online issue, which is available at wileyonlinelibrary.com]

in Figure 1, where a_1 indicates the new width of the middle part of the filter. It affects the lower cutoff frequency (f_c^1) of the passband in such a way that a decrease in a_1 moves f_c^1 toward the higher frequency side, and vice versa. Additionally, it improves the matching within the passband.

The second additional control mechanism is to introduce overall four additional vias at the input and output sides of the filter (two at one side and two at the other side) as shown in Figure 1. At each side, the two additional vias are aligned with the first/last vias of the SIW's wall and the separation between these two vias is a_2. These additional vias (and hence, the size of a_2) improves the lower frequency suppression, thereby establishing a symmetric filter response. Besides, they have an influence on the matching of the filter as well. Hence, the separation a_2 is optimized for the best matching.

For the third-order design shown in Figure 1, using CST MWS and making use of [14], the unloaded Q-factor of a single resonator is calculated approximately 290 at 9 GHz including dielectric and conductor losses.

Rogers TMM10i that has a thickness of 0.635 mm, $\varepsilon_r = 9.8$ and loss tangent 0.002 (at 10 GHz) is used for the fabrication of the proposed filter, and copper is used for its conducting parts. The dimensions of the third-order fabricated prototype filter, shown in Figure 1, together with its tapered microstrip-to-SIW transition are given in Table 1. All metallic vias have standard diameter of 0.4 mm, and the center-to-center distance between two successive vias is 0.711 mm. Finally, the width of the 50 Ω line is 0.56 mm and the gap width of each annular gap around the cap is 0.254 mm (as mentioned before). The fabricated filter is placed in a box to minimize radiation effects, and is measured using Southwest Microwave's end-launch SMA connectors due to their easy integration and low loss around the operating frequency of 9 GHz. Figure 3 shows the comparison of measured and simulated S-parameters (i.e., S_{11} and S_{21}) results. Good agreement is obtained in the results. However, the measured 2 dB insertion loss is higher than that of simulated which is 1.3 dB. The 0.7 dB difference in the insertion loss can be attributed to the connector losses, as well as some unpredicted losses due to materials used to construct the prototype.

3. HARMONIC SUPPRESSION AND FINAL DESIGN

One problem with the design is that the filter exhibits a higher order harmonic around 13.5 GHz (i.e., 1.5 f_0) as shown in Figure 4. Therefore, three dumbbell shaped slots (DSS) are introduced to the ground side of the microstrip line feeding sections

TABLE 1 Dimensions of the Prototype Filter Shown in Figure 1

Parameter	Length (mm)	Parameter	Length (mm)
w_t	2.54	l_t	8.382
d_1	2.807	d_2	2.743
a_1	5.69	a_2	4.978
a_s	7.214	l_1	2.54

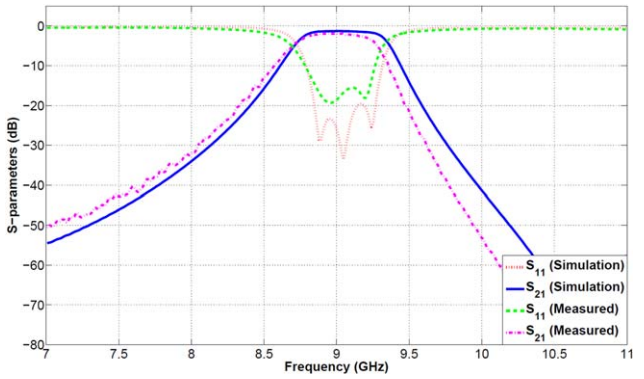

Figure 3 Simulated and measured *S*-parameter results for the third-order prototype filter depicted in Figure 1. [Color figure can be viewed in the online issue, which is available at wileyonlinelibrary.com]

at both ends of the filter to suppress this harmonic. All dumbbells are identical, and each dumbbell has two square-shaped heads (length of which is labeled with h) separated by a long slot with a length L and width w as shown in Figure 5. The size of the dumbbell heads (i.e., h) affects the matching, the length of the long slot (separating the heads and labeled as L) determines the frequency to be suppressed, and the separation between the dumbbells is optimized for the best performance. Note that with a single and/or two dumbbells at each side, the matching is not sufficient. Conversely, making use of more dumbbells increases the complexity of the design resulting higher loss. Figure 6 shows the top and bottom surfaces of the final design, a photograph of the fabricated third-order SIW-based interdigital filter in the presence of the DSS (on the ground side of the microstrip feeding section at both ends) for the final dimensions given in Table 2 together with the box in which the final prototype is placed. Figure 7 shows the comparison of measured and simulated S_{11} and S_{21} results for the final design depicted in Figure 6 whereas Figure 8 illustrates the effect of the DSS on the higher order harmonic around 13.5 GHz by comparing the measured *S*-parameters of the prototype filters depicted in Figure 1 (without DSS) and Figure 6 (with DSS). As seen from the measurement results, the harmonic at 13.5 GHz is suppressed more than 30 dB with still maintaining a good matching at the operating frequency of 9 GHz with a 500 MHz bandwith. However, it should be noted that the length of the transtions is increased as a consequence of the dumbbells resulting an additional 0.3 dB insertion loss compared to the same design without the dumbbells.

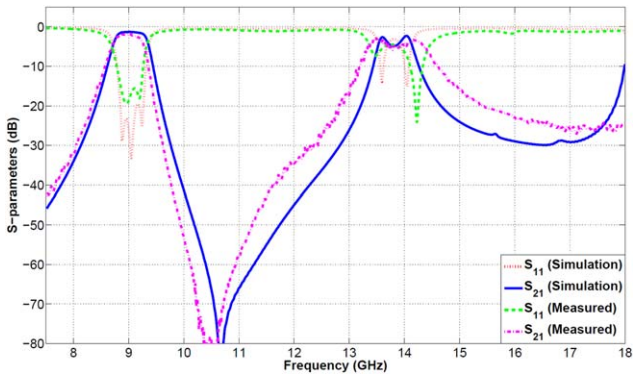

Figure 4 Harmonic response for the third-order prototype filter depicted in Figure 1. [Color figure can be viewed in the online issue, which is available at wileyonlinelibrary.com]

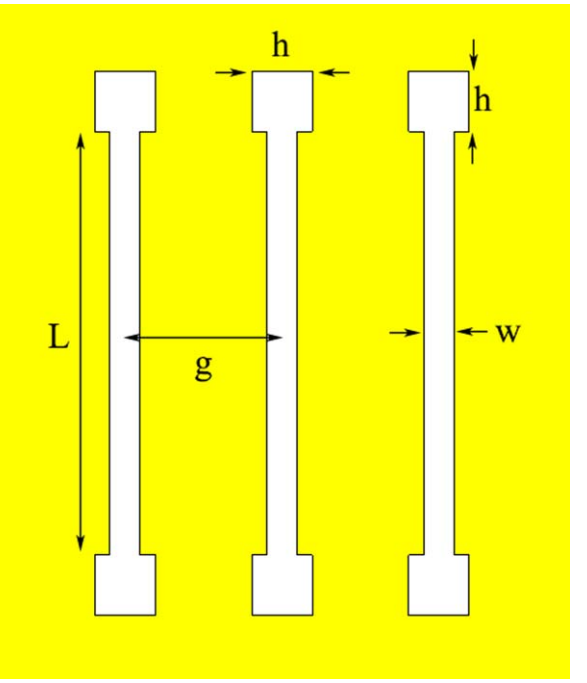

Figure 5 Parameters of the three DSS etched to the ground. [Color figure can be viewed in the online issue, which is available at wileyonlinelibrary.com]

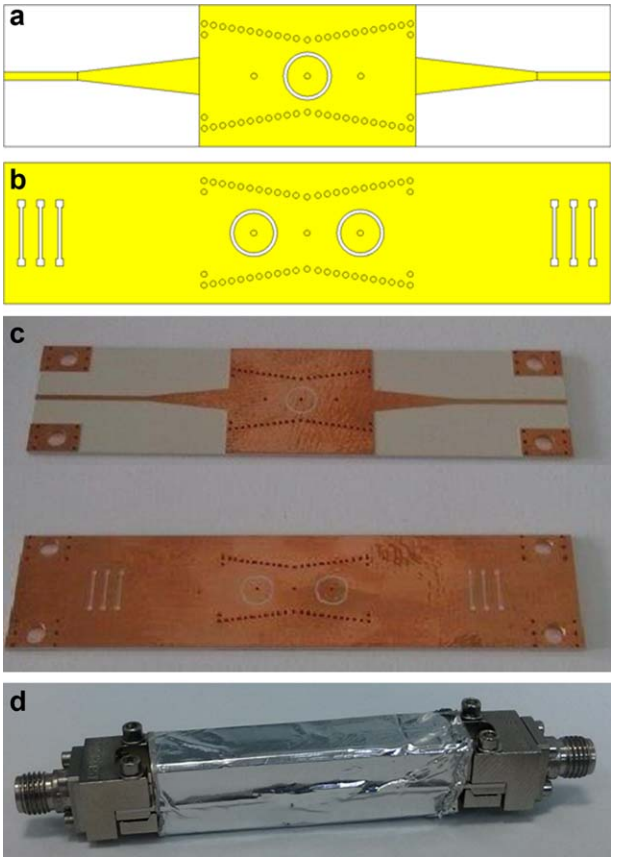

Figure 6 The final structure of the proposed filter together with its fabricated prototype. (a) Top surface, (b) bottom surface, (c) top and bottom surfaces of the fabricated prototype, (d) the box (used in measurements) in which the filter, shown in (c), is placed. [Color figure can be viewed in the online issue, which is available at wileyonlinelibrary.com]

TABLE 2 Dimensions of the Final Prototype Filter with Dumbbell DGS Etched

Parameter	Length (mm)	Parameter	Length (mm)
w_t	2.54	l_t	8.382
d_1	2.807	d_2	2.743
a_1	5.69	a_2	4.978
a_s	7.214	l_1	2.54
L	3.556	g	1.32
h	0.508	w	0.254

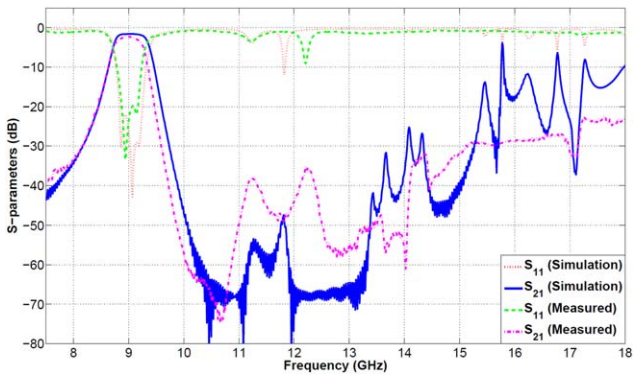

Figure 7 Simulated and measured *S*-parameter results for the final third-order prototype filter with DSS depicted in Figure 6. [Color figure can be viewed in the online issue, which is available at wileyonlinelibrary.com]

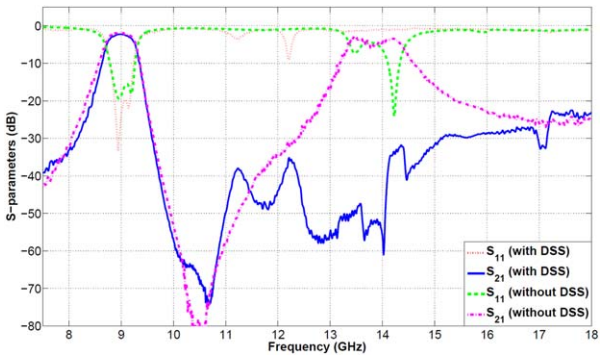

Figure 8 Measured harmonic performance of the third-order prototype filters with and without DSS. [Color figure can be viewed in the online issue, which is available at wileyonlinelibrary.com]

4. CONCLUSION

A novel SIW-based interdigital BPF is presented. In addition to the interdigital SIW resonators, two additional control mechanisms, namely narrowing the width of the SIW at the middle of filter and use of additional vias at its input and output sides, are introduced to achieve the desired response. The proposed structure is verified with a fabricated prototype which exhibits good filtering properties and good harmonic suppression due to the DSS etched to the ground side of the microstrip line feeding section at both ends of the filter.

REFERENCES

1. G.L. Matthaei, Combline band-pass filters of narrow or moderate bandwidth, Microwave J 6 (1963), 82–91.
2. G. Matthaei, E.M.T. Jones, and L. Young, Microwave filters, impedance-matching networks, and coupling structures, Artech House, Norwood, MA, 1980.
3. M. Bozzi, A. Georgiadis, and K. Wu, Review of substrate-integrated waveguide circuits and antennas, IET Microwave Antennas Propag 5 (2011), 909–920.
4. J.E. Rayas-Sanchez, An improved em-based design procedure for single layer substrate integrated waveguide interconnects with microstrip transitions, In: IEEE MTT-S International Microwave Workshop Series on Signal Integrity and High Speed Interconnects, Guadalajara, Mexico, February 2009.
5. X.-P. Chen and K. Wu, Substrate integrated waveguide cross-coupled filter with negative coupling structure, IEEE Trans Microwave Theory Tech 56 (2008), 142–149.
6. B. Potelon, J.-F. Favennec, C. Quendo, E. Rius, C. Person, and J.-C. Bohorquez, Design of a substrate integrated waveguide (SIW) filter using a novel topology of coupling, IEEE Microwave Wireless Comp Lett 18 (2008), 596–598.
7. T.-S. Yun, H. Nam, K.-B. Kim, and J.-C. Lee, Iris waveguide bandpass filter using substrate integrated waveguide (siw) for satellite communication, In: Asia-Pacific Microwave Conference Proceedings, Suzhou, China, 2005.
8. Y.D. Dong, T. Yang, and T. Itoh, Substrate integrated waveguide loaded by complementary split-ring resonators and its applications to miniaturized waveguide filters, IEEE Trans Microwave Theory Tech 57 (2009), 2211–2223.
9. Y.L. Zhang, W. Hong, K. Wu, J.X. Chen, and H.J. Tang, Novel substrate integrated waveguide cavity filter with defected ground structure, IEEE Trans Microwave Theory Tech 53 (2005), 1280–1287.
10. K. Deng, Z. Guo, C. Li, and W. Che, A compact planar bandpass filter with wide out-of-band rejection implemented by substrate-integrated waveguide and complementary split-ring resonator, Microwave Opt Technol Lett 53 (2011), 1483–1487.
11. J.C. Bohórquez, B. Potelon, C. Person, E. Rius, C. Quendo, G. Tanńe, and E. Fourn, Reconfigurable planar SIW cavity resonator and filter, In: IEEE MTT-S International Microwave Symposium Digest 2006, San Francisco CA, pp. 947–950.
12. J.D. Martinez, M. Taroncher, and V.E. Boria, Capacitively loaded resonator for compact substrate integrated waveguide filters, In: Proceedings of 40th European Microwave Conference, Paris, France, 2010, pp. 192–195.
13. J.D. Martinez, S. Sirci, and V.E. Boria, Compact cpw-fed combline filter in substrate integrated waveguide technology, IEEE Microwave Wireless Comp Lett 22 (2012), 7–9.
14. D. Kajfez, Q-factor, Oxford, MS, Vector Forum, 1994.

A COMPACT MODIFIED TRIANGULAR CPW-FED ANTENNA WITH MULTIOCTAVE BANDWIDTH

Amir Siahcheshm,[1] Javad Nourinia,[1] Yashar Zehforoosh,[2] and Bahman Mohammadi[1]
[1] Department of Electrical Engineering, Urmia University, Urmia, Iran; Corresponding author: b.mohammadi@urmia.ac.ir
[2] Department of Electrical Engineering, Urmia Branch, Islamic Azad University, Urmia, Iran

Received 9 June 2014

ABSTRACT: *This article presents the results of a compact modified triangular CPW-fed antenna that exhibits multioctave performance. This modification significantly improves the antenna's impedance bandwidth by 198% over an ultra-wideband (UWB) frequency range from 3.06 to 35 GHz. The return-loss (S_{11}) performance over this frequency range is designed to be better than −10 dB. These characteristics make the proposed antenna an excellent candidate for numerous UWB applications and next generation communication systems. The key physical parameters affecting the antenna's frequency characteristics have also been*